Int. J. Electrochem. Sci., 11 **(2016)** 8875 – 8891, doi: 10.20964/2016.11.42

International Journal of
ELECTROCHEMICAL
SCIENCE
www.electrochemsci.org

Electrochemical Ozone Generation on a Nanocomposite SnO_2 Electrode

Yu-Hong Cui[*], *Jing-Ya Feng*, *Cong-Jian Fan and Zheng-Qian Liu*[*]

School of Environmental Science and Engineering, Huazhong University of Science and Technology, No. 1037 Luoyu Road, Hongshan District, Wuhan 430074, P. R. China.
[*]E-mail: yhcui@hust.edu.cn; zhengqianliu@126.com

Received: 1 July 2016 / *Accepted:* 10 September 2016 / *Published:* 10 October 2016

A nanocomposite SnO_2 electrode was prepared and its performance on electrochemical ozone synthesis was studied. The factors affecting ozone production and its current efficiency, such as current density, temperature, pH, supporting electrolyte and liquid flow, were investigated. The formation of hydroxyl radical was detected using trapping protocol and was compared with ozone generation. The results indicate that the ozone production increases with current density, and an optimum current density of 5 mA cm^{-2} is obtained for the current efficiency of ozone generation. Lower temperature, lower pH and higher liquid flow favor ozone production as well as its current efficiency. As a supporting electrolyte, Na_2SO_4 appears to be more suitable than $NaClO_4$, $NaNO_3$ and NaCl for ozone generation on the nanocomposite SnO_2 electrode. An optimum electrolyte concentration of Na_2SO_4 is observed to be 0.25 M, and a little bit of KPF_6 addition (0.01 - 0.05 M) has an obviously positive effect on ozone generation. Current density and solution pH have a coincident effect on ozone and hydroxyl radical generation, while temperature has an inconsistent effect on ozone and hydroxyl radical generation and KPF_6 addition has no effect on hydroxyl radical generation on the nanocomposite SnO_2 electrode. The morphology and structure of the nanocomposite SnO_2 electrode before and after accelerated life test were characterized by SEM and XRD analysis. It is suggested that the deactivation of nanocomposite SnO_2 electrode is caused by the destruction of SnO_2 coating film and the growth of TiO_2 between Ti-base and SnO_2 coating film.

Keywords: Ozone; hydroxyl radical; SnO_2 electrode; deactivation

1. INTRODUCTION

Ozone has been widely used in health, food, chemical and other fields; it also gets widely application in water and wastewater treatment [1, 2]. The traditional method of producing ozone is by high voltage cold corona discharge which synthesis ozone from air or oxygen. But this method has some disadvantages such as nitrogen oxide formation and complex equipment. Besides, when ozone is

used for water and wastewater treatment, ozone loss and decay always existed during the transfer process from gaseous ozone to dissolved ozone [3]. Therefore, electrochemical synthesis of ozone directly by water electrolysis gets much attention in recent years [3, 4, 5]. The concentration of ozone in water produced by electrochemical synthesis could be as high as 34 mg/L [6], which is much higher than that of the one produced by corona discharge.

The electrode materials are critical on the effectiveness of electrochemical ozone production. Since oxygen generation is the main competing reaction (shown in equation 1 and 2), an anode with high oxygen evolution potential is necessary in the electrochemical ozone generation process as high oxygen evolution potential can cut down the current ratio on oxygen generation.

$$3H_2O \rightarrow O_3 + 6H^+ + 6e^- \quad (E^0=1.51\ V) \qquad (1)$$

$$2H_2O \rightarrow O_2 + 4H^+ + 4e^- \quad (E^0=1.23\ V) \qquad (2)$$

Platinum was used for ozone generation in the early research, but its application was limited due to the high cost and the low efficiency (< 5%) at mild conditions [7]. Lead dioxide (PbO_2) was the most investigated electrode material in the last decades for electrochemical ozone generation and about 10-20% current efficiency could be obtained at room temperature [4, 8]. The morphology and structure as well as the factors affecting electrochemical ozone generation on PbO_2 electrodes have been investigated [8, 9, 10, 11]. Some researchers also discussed the mechanism of ozone generation on PbO_2 anode surface which involves hydroxyl radicals ($^{\bullet}OH$) and adsorbed oxygen atoms ($^{\bullet}O_{ads}$) [12, 13]. Other electrode materials have been examined such as Ti-based or Si-based metal/metal oxides (e.g. Ti/Pt-TaO_x [14], Si/TiO_x/Pt/TiO_2 [14], Ti/IrO_2-Nb_2O_5 [15], Ti/Ni-Sb-SnO_2 [3, 6]) and boron doped diamond (BDD) electrode [17, 18]; while the mechanism of ozone generation on these electrodes are seldom mentioned.

Because of the high oxygen evolution potential (>1.7 V vs. SCE) and the low cost, the doped SnO_2 electrode becomes one of the most promising electrode materials concerning electrochemical ozone generation. High ozone concentration (34 mg/L) in aqueous solution and high current efficiency (36-50%) for ozone production were achieved at room temperature on the Ni and Sb co-doped SnO_2 anode [6, 19, 20]. It has been reported that the enrichment of Ni element on the Ni-Sb-SnO_2 electrode surface should be responsible for the high ozone productivity [21]. However, the mechanism of ozone formation on the SnO_2 electrode surface still need to be further investigated.

It should be pointed out that the SnO_2 electrode shows excellent performance on degradation of organic pollutants in water and wastewater treatment due to its efficiency on hydroxyl radical ($^{\bullet}OH$) generation which can oxidize organics almost nonselectively [22, 23, 24]. Actually, the most promising electrode materials on electrochemical ozone generation, namely PbO_2, SnO_2 and BDD electrodes, are also the most promising electrode materials on organics degradation in water and wastewater treatment, and their superiority on organics removal benefit from their capacity of $^{\bullet}OH$ generation through water electrolysis [25, 26, 27]. Therefore, it is reasonable to speculate that there may have some relationship between ozone and $^{\bullet}OH$ production for a certain electrode. Though there are some discussion on electrochemical ozone generation/decomposition and $^{\bullet}OH$ formation in the processes of organics removal [28, 29], there is few report focused on ozone and $^{\bullet}OH$ formation on a typical electrode such as SnO_2 electrode.

In this research, we prepared a nanocomposite SnO_2 electrode and studied the electrode's performance on electrochemical synthesis of ozone. The factors affecting ozone generation and conversion, such as current density, temperature, pH, electrolyte and mass transfer process, were investigated. The formation of $^{\bullet}OH$ was detected and the relationship between ozone and $^{\bullet}OH$ generation was discussed. Finally, the electrode deactivation mechanism was analyzed based on the electrode characteristics before and after accelerated life test.

2. EXPERIMENTAL

2.1 Preparation of electrode

The nanocomposite SnO_2 electrode was prepared as previously described [30], including TiO_2 nanotube preparation and the preparation of inner layer and outer layer coatings. The Ti plate (2 cm × 2 cm) was polished with 360-grit, 800-grit, 1000-grit and 1500-grit sand papers, degreased in 40% NaOH at 80 ^{o}C for 2 h, and etched in 10% boiling oxalic acid for 2 h. After thorough washing with deionized water, the pretreated Ti plate was anodized for 2 h in a two-electrode system with a platinum foil as counter electrode and the cell voltage was kept on 20 V. This anodization is to obtain TiO_2 nanotubes on the Ti plate surface and it was carried out in an electrolyte solution of Na_2SO_4 (0.1 M) and NaF (0.2 M) with deionized water and polyethylene glycol (volume ratio of 10 : 90) as solvents. The obtained TiO_2 nanotubes on the Ti plate are cleaned by ethanol and deionized water. Then an inner layer was prepared by alternate cathodic deposition of Sn and Sb into the TiO_2 nanotubes with 0.2 M $SnCl_2$ citric acid solution and 0.1 M $SbCl_3$ citric acid solution at a constant current density of 10 mA cm^{-2}. The electro-deposition time was controlled as 170 s for Sn deposition and 12 s for Sb deposition, respectively. The above deposition procedures were repeated for 5 times and the electrode was thermal treated at 400 °C for 1 h in a muffle oven. The preparation of this inner layer has two advantages. One is that the TiO_2 nanotubes could be better filled than by the method of directly dip-coating; the other is that the metal/metal oxide particles growing from electro-deposition is more uniform and facilitated the following preparation of the outer layer [30]. The active outer layer of the electrode was obtained by a traditional dip-coating procedure, which includes dipping in an alcohol solution composed of 1.0 M $SnCl_4{\cdot}5H_2O$, 0.016 M $SbCl_3$, and 0.002 M $NiCl_2{\cdot}6H_2O$, drying at 80 ^{o}C and heating at 400 ^{o}C for 10 min. After more than twenty cycles of dipping, drying and pyrolysis, the electrode was heated at 550 ^{o}C for 3 h. So far the nanocomposite SnO_2 electrode was obtained.

2.2 Electrochemical ozone generation and ozone measurement

The electrochemical ozone generation experiments were conducted in an H-type cell which has an anode chamber and a cathode chamber separated by a Nafion 117 membrane. The prepared nanocomposite SnO_2 electrode was fixed in the anode chamber and a Ti electrode with a same area was fixed in the cathode chamber. Both the anode chamber and the cathode chamber contained 80 mL of electrolyte. In the anode chamber, the electrolyte flowed into the chamber from the bottom and

flowed out from the top of the chamber. An electro-thermostatic water bath was applied to control the electrolyte temperature during the electrolysis. Thus, the electrolyte in the cathode chamber did not flow and the results were not affected. The concentrated H_2SO_4 (or HCl, HNO_3, $HClO_4$, depending on the anion of the electrolyte used in the experiments) solution and the concentrated NaOH solution were used to adjust the pH of the electrolyte. KPF_6 was selected to provide special anion (PF_6^-) in some experiments. A computer-controlled potentiostat/galvanostat (CS-350, Corrtest) was used to supply a constant current.

The electrolyte from the outlet of the anode chamber was immediately removed and measured by UV adsorption at 258 nm with an UV-visible spectrophotometer (UV-1800, Mapata) and the dissolved ozone concentration was calculated based on a molar absorption coefficient of 2900 L mol^{-1} cm^{-1} [3]. The length of the light path in the present experiments is 1 cm. The ozone production can be calculated as

$$\mathrm{P} = \frac{cq \times 60}{1000} \quad (3)$$

where P is the dissolved ozone production (mg min^{-1}), *c* is the concentration of dissolved ozone (mg L^{-1}) and *q* is the electrolyte supply (mL s^{-1}).

The current efficiency for electrochemical ozone generation can be calculated as

$$CE = \frac{nFcq}{48 \times 10^6 \times I} \times 100\% \quad (4)$$

where *n* represents the moles of electrons for one mole of ozone production in the electrochemical process and is equal to 6, *F* is the Faraday constant (96485 C mol^{-1}) and *I* is the applied current (A).

2.3 Examination of hydroxyl radical

The $^{\bullet}OH$ examination experiments were conducted in the same H-type cell as in the ozone generation experiments. For convenience, the $^{\bullet}OH$ production in the anode chamber was measured without electrolyte flow. A terephthalic acid trapping protocol was used to identify the $^{\bullet}OH$ generated in the electrolytic system. Briefly, the terephthalic acid with a concentration of 0.5 mM was added into the electrolyte as a quenching agent before the electrolysis. When the electrolysis turned on, the electrochemical generated $^{\bullet}OH$ would be trapped by the non-fluorescent terephthalic acid to form 2-hydroxyterephthalate acid which is highly fluorescent. The concentration of 2-hydroxyterephthalate acid was determined every five minutes by the fluorescence intensity at 425 nm using a fluorescence spectrophotometer (F-4600, Hitachi) with excitation at 315 nm [30, 31].

2.4 Service life test and the characterization of the electrode

An accelerated service life test of the nanocomposite SnO_2 electrode was conducted in the same H-type cell. Considering that the frequently-used current density of the nanocomposite SnO_2 electrode is 5 mA/cm^2 (see Figures), the accelerated life test was fixed at a current density of 50

mA/cm^2 to avoid high distortion. The electrolyte was 0.25 M Na_2SO_4 and the solution pH was adjusted to be 2.0.

The morphology of the prepared electrode before and after service life test was analyzed using a field-emission scanning electron microscope (FESEM) (Quanta 450 FEG, FEI/Philips). The structure of the electrode before and after service life test was analyzed by an X-ray diffraction (XRD) instrument (X'Pert PRO, PANalytical B.V.), using Cu Kα radiation (λ = 0.15406 nm), with an operating voltage of 40 kV and current of 40 mA.

3. RESULTS AND DISCUSSION

3.1 Factors affecting ozone generation on the nanocomposite SnO_2 anode

3.1.1 The effect of supporting electrolytes

Some researchers found that ozone generation efficiency differs in different supporting electrolytes and at different concentrations [6, 12, 32]. In Fig. 1, we investigated the effect of electrolyte type on ozone production and current efficiency on the nanocomposite SnO_2 electrode. Exclude the same type of cation, the type of anion has a remarkable effect on ozone generation in the present study. The highest ozone production and current efficiency are achieved in Na_2SO_4, followed in $NaClO_4$ and $NaNO_3$, and the lowest ozone production and current efficiency are obtained in NaCl electrolyte.

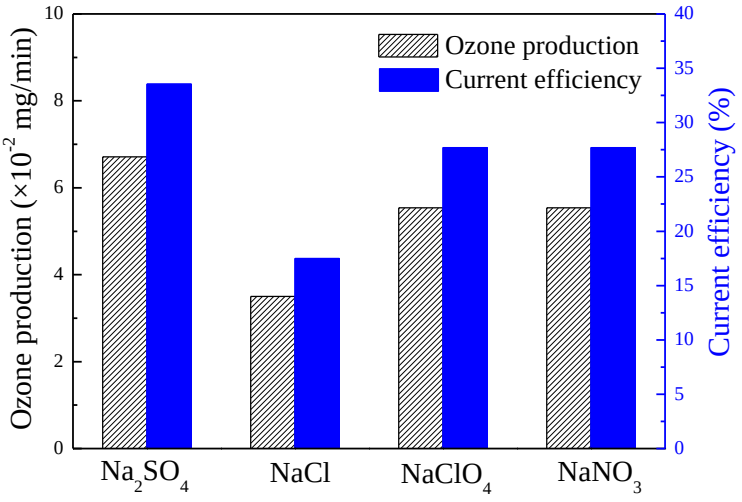

Figure 1. Effect of electrolyte type on ozone production and current efficiency. Electrolyte concentration = 0.25 mol/L, electrolyte supply = 4.8 mL/s, current density = 5 mA/cm^2, temperature = 25 ^oC, pH = 2.

Wang et al. [6] have studied Sb–Ni-doped SnO_2 electrode in H_2SO_4, $HClO_4$ and H_3PO_4 with different electrolyte concentrations, and the highest efficiency on ozone production was achieved in H_2SO_4. They believed that SO_4^{2-} has stronger adsorption which is helpful to intermediate steps of the reaction. For the nanocomposite SnO_2 electrode as in the present study, the different effect of the electrolyte on ozone generation should be caused by the different stability and adsorption capacity of the anions, as Cl^- is easily oxidized which cause loss of current and SO_4^{2-} is more electronegative and has stronger adsorption on the anode surface [4].

3.1.2 The effect of supporting electrolyte concentration

The concentration of electrolyte directly affects ozone production and current efficiency on the nanocomposite SnO_2 electrode, as shown in Fig. 2. When Na_2SO_4 concentration is lower than 0.25 M, the ozone production and the current efficiency increase with electrolyte concentration. After reaching the maximum value, the ozone production rate and the current efficiency decrease with electrolyte concentration increase.

The electrolyte conductivity increases with electrolyte concentration which induces more active sites on the anode surface and results higher ozone production as well as current efficiency. However, the more active sites mean the increase of the active anode area which leads to lower real current density though the apparent current density keeps constant [33]. The lowered real current density may cause lower ozone generation efficiency (as shown in Fig. 4). In the present work, the two opposite effects as above mentioned lead to the results as observed in Fig. 2. Besides, it should be pointed out that the increase of electrolyte concentration can lower the cell voltage. Thus, the increase of electrolyte concentration can be a resolution if energy consumption had to be considered.

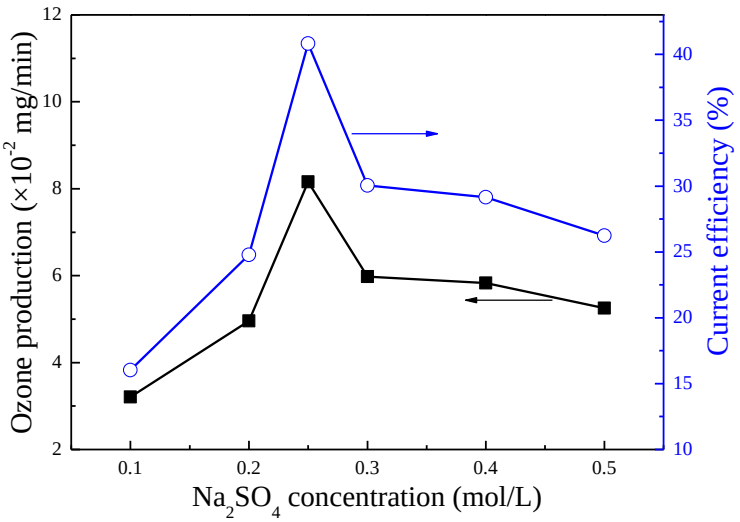

Figure 2. Effect of Na_2SO_4 concentration on ozone production and current efficiency. Electrolyte supply = 4.8 mL/s, current density = 5 mA/cm^2, temperature = 5 ^{o}C, pH = 2.

3.1.3 The effect of electrolyte supply

The effect of electrolyte supply on ozone production and current efficiency on the nanocomposite SnO_2 electrode is shown in Fig. 3. Both ozone production and current efficiency increase with electrolyte supply, especially at low flow rate (less than 5 mL/s). The similar tendency has been also found in ozone generation experiments with PbO_2 electrode [34] and Sb–Ni-doped SnO_2 electrode [3]. Ozone is unstable and can decompose to oxygen. The increased flow rate can lower the concentration of dissolved ozone in water and reduce the decomposition rate of ozone to oxygen (shown in equation 5).

$$2O_3 \rightarrow 3O_2 \quad (5)$$

Furthermore, the increased water flow removes the products (e.g. ozone and oxygen) near the anode surface which improves mass transfer of the electrochemical reaction on ozone and oxygen generation [3]. Additionally, a reduced cell voltage is observed with the increasing of electrolyte supply. This may benefit from the forced convection which can prevent bubbles (ozone or oxygen) accumulation. Thus, a sufficient electrolyte supply would favor ozone production especially aqueous ozone production.

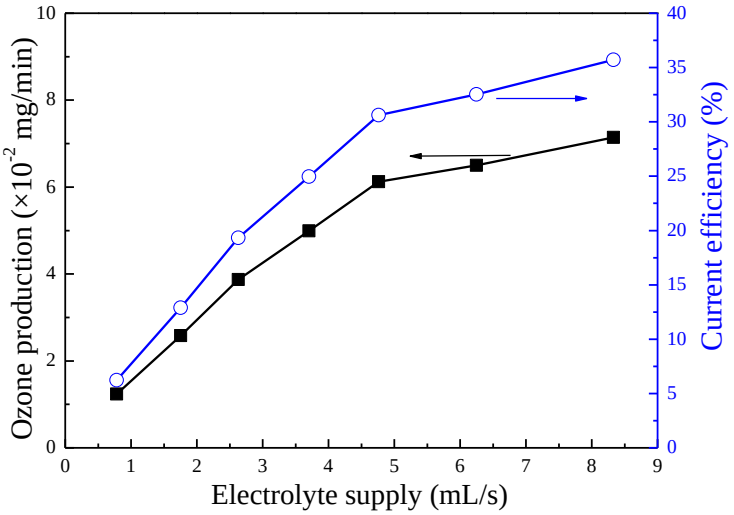

Figure 3. Effect of electrolyte supply on ozone production and current efficiency. Na_2SO_4 concentration = 0.25 mol/L, current density = 5 mA/cm^2, temperature = 25 ^{o}C, pH = 2.

3.1.4 The effect of current density

Ozone production increases with current density, as anticipated, while a loss of current efficiency is observed when the current density is higher than a certain value (5 mA/cm^2), as shown in Fig. 4a. Onda et al. [34] and Wang et al. [35] have reported a similar effect of current density on ozone generation efficiency with PbO_2 electrode and Sb–Ni-doped SnO_2 electrode, but the optimal value of

current density is 1.0 A/cm^2 and 12.5 mA/cm^2, respectively. The difference of the optimal current density between the present research and previous studies should be due to different materials and different surface structure (e.g. surface roughness which affect the ratio of real current density vs. apparent current density) of the electrodes.

The variation of current efficiency could be explained as follows. Ozone generation (shown in equation 1) and oxygen generation (shown in equation 2) are parallel reactions in water electrolysis. The standard equilibrium potential of ozone evolution (1.51 V vs RHE) is higher than that of oxygen evolution (1.23 V vs RHE). Hence, it is difficult for ozone generation at a very low potential (corresponding to a small current density) compared with oxygen generation. With the increase of current density, ozone generation happens and is relatively higher. That is why the current efficiency for ozone production increases with current density when it is lower than 5 mA/cm^2. However, the change of current density may have different effects on ozone generation and oxygen generation. An increased concentration of dissolved ozone may cause an increased decomposition of ozone to oxygen (shown in equation 5) since ozone is unstable. Moreover, some researchers have found that the adsorbed ozone molecules would replace some key adsorbed intermediates (e.g. adsorbed $^{\bullet}$OH or $^{\bullet}$O) on the anode surface and inhibit ozone generation [36]. Therefore, with further increase of current density, the current efficiency for ozone production decreases.

The fluorescence intensity of the electrolyte was recorded by using terephthalic acid as a quenching agent to show the effect of current density on $^{\bullet}$OH generation on the nanocomposite SnO_2 electrode (as shown in Fig. 4b). The fluorescence intensity increases with time, indicating a $^{\bullet}$OH generation with electrolysis. The decrease of fluorescence intensity at 20 mA/cm^2 after 15 min's electrolysis should be due to the over consumption of terephthalic acid. Considering the rising rate and intensity of fluorescence intensity at different current densities (in 15 min's electrolysis), Fig. 4b clearly shows that the increase of current density favors the fluorescence intensity, which is in agreement with that of ozone production (Fig. 4a). This result indicates that $^{\bullet}$OH generation and ozone production have positive correlation in the present electrochemical system.

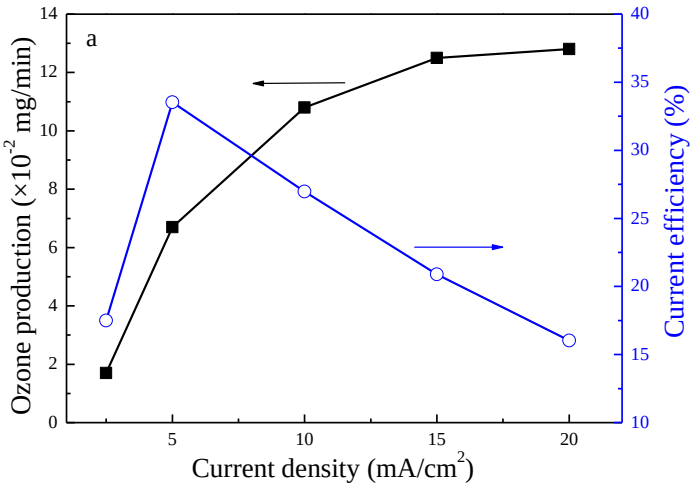

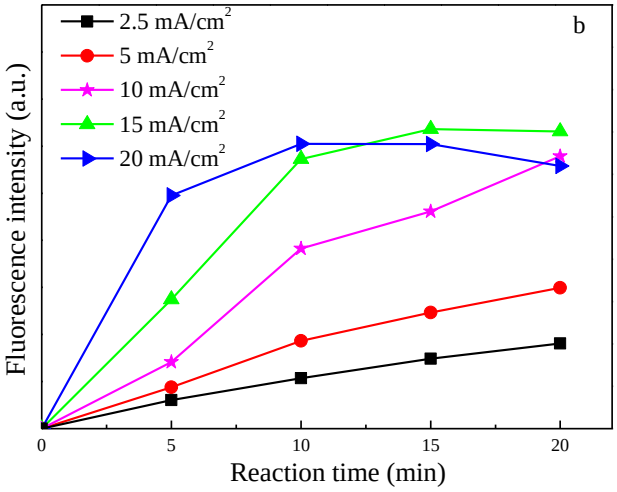

Figure 4. Effect of current density on (a) ozone production and current efficiency (electrolyte supply = 4.8 mL/s, pH = 2), (b) hydroxyl radical generation. Na_2SO_4 concentration = 0.25 mol/L, temperature = 25 ^oC.

3.1.5 The effect of temperature

The effect of temperature on ozone production and current efficiency on the nanocomposite SnO_2 electrode is shown in Fig. 5a. Increasing the electrolyte temperature from 5 ^oC to 45 ^oC causes continuously reductions of both ozone production and current efficiency, especially at temperatures above 25 ^oC. This result is something different from previous research on PbO_2 anode [34], in which an optimal temperature of 25 ^oC is observed. Though a temperature rise favors electrochemical reaction kinetics, it would accelerate the ozone decomposition (as shown in equation 5) in aqueous solution.

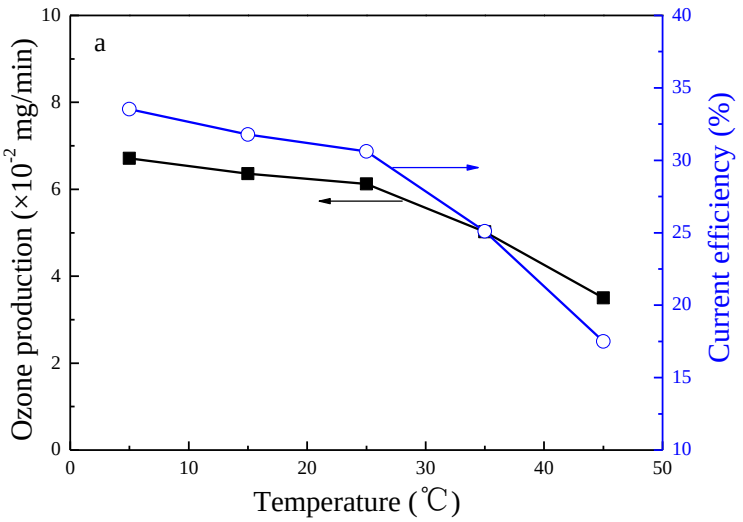

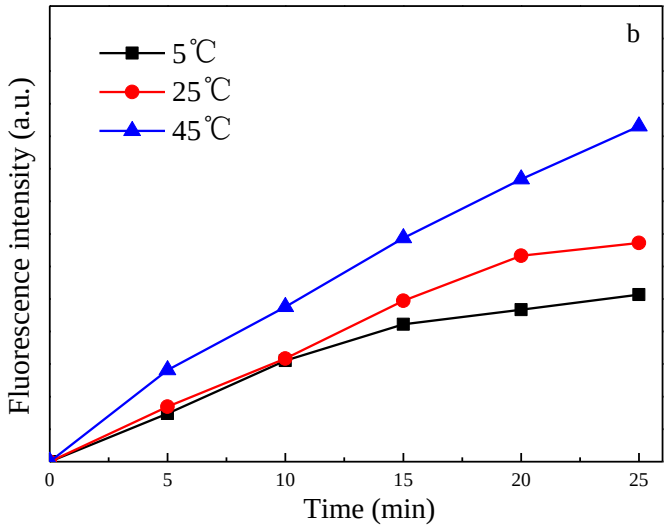

Figure 5. Effect of temperature on (a) ozone production and current efficiency, (electrolyte supply = 4.8 mL/s, pH = 7), (b) Effect of temperature on hydroxyl radical generation. Na_2SO_4 concentration = 0.25 mol/L, current density = 5 mA/cm^2.

Besides, some researchers have argued that a high temperature can reduce the surface coverage by oxygenated species on PbO_2 anode which is essential in ozone synthesis [12]. It seems that the negative effect exceeds the positive effect of temperature on ozone generation for the nanocomposite SnO_2 electrode. Therefore, a high temperature is unfavorable for electrochemical generation of dissolved ozone in the present study.

The effect of temperature on hydroxyl radical generation on the nanocomposite SnO_2 electrode is shown in Fig. 5b. A temperature rise promotes the $^{\bullet}OH$ production. As aforementioned, the temperature rise favors electrochemical kinetics which is helpful for the $^{\bullet}OH$ generation on anode surface. Additionally, a high temperature favors the mass transfer process of generated $^{\bullet}OH$ from anode surface to bulk solution, which would contribute to the trapping reaction of trapping agent with $^{\bullet}OH$ to form more fluorescent substances. More importantly, the temperature increase would accelerate ozone decomposition and $^{\bullet}OH$ is an important intermediate products in aqueous ozone decomposition. All of the above factors lead to an increased $^{\bullet}OH$ production with temperature rise.

3.1.6 The effect of solution pH

Fig. 6a shows the effect of solution pH on electrochemical ozone generation on the nanocomposite SnO_2 electrode.

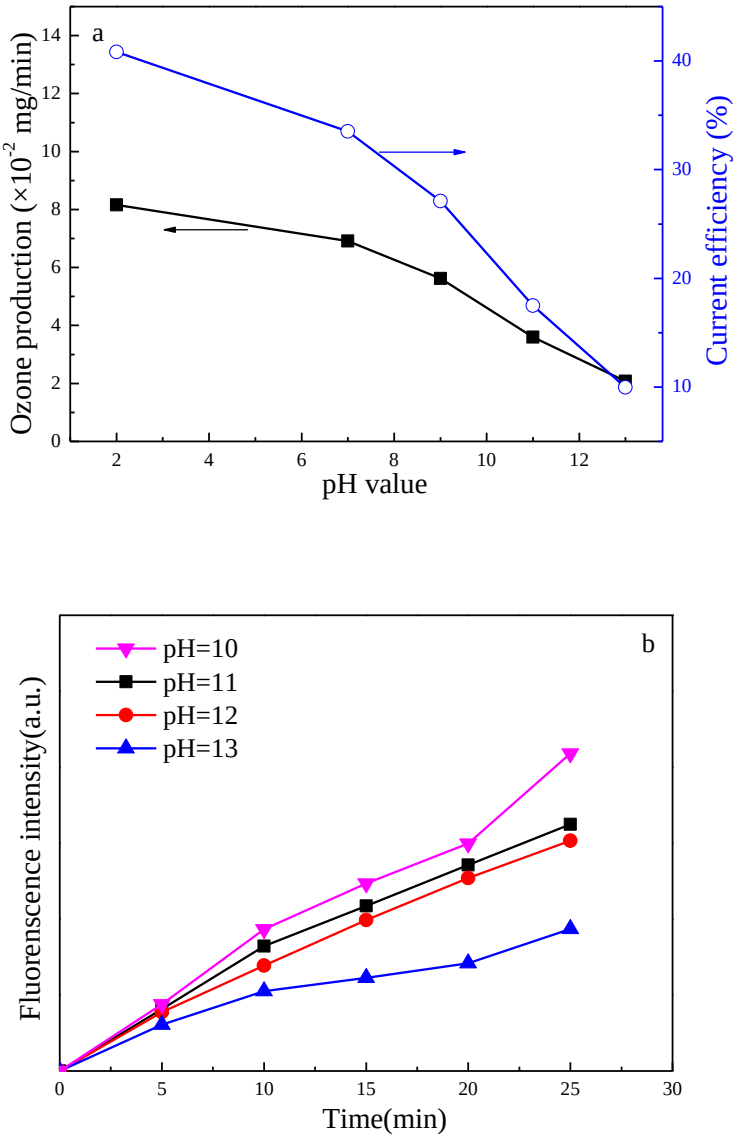

Figure 6. Effect of pH on (a) ozone production and current efficiency (electrolyte supply = 4.8 mL/s), (b) Effect of pH on hydroxyl radical generation. Na_2SO_4 concentration = 0.25 mol/L, current density = 5 mA/cm^2, temperature = 5 ^oC.

It is clearly that the acidic electrolyte is benefit to both ozone production and current efficiency, while the basic electrolyte is not good for ozone generation. Ozone is well known to be an unstable chemical and it is more ready to decompose (as shown in equation 5) in aqueous solution at high pH. Thus, the observed ozone production and current efficiency would be depressed with pH increase. Besides, our previous study has found that the oxygen evolution potential of the nanocomposite SnO_2 electrode would be lower in a basic electrolyte than that in an acidic electrolyte [30], and low oxygen evolution potential is not good for the ozone generation.

The effect of pH on $^{\bullet}OH$ generation is difficult to be investigated since the trapping agent of terephthalic acid is insoluble in neutral and acidic solutions. However, in basic solutions with a pH range from 10 to 13, the $^{\bullet}OH$ production decreases with the increasing of pH (Fig. 6b). It is well

known that the electrode material with a high oxygen evolution potential favors $^{\bullet}OH$ generation [24, 25, 26, 27] and this potential has been proved to be higher in an acidic solution for the nanocomposite SnO_2 electrode [30]. Thus, it can be speculated that more $^{\bullet}OH$ would be generated in an acidic solution which is in agreement with that of ozone production.

3.1.7 The effect of KPF_6 addition

Some researchers have found that the addition of special anions like F^-, BF_4^- and PF_6^-, can promote ozone production on PbO_2 anode [11, 37]. In the present study, KPF_6 was selected as additive and the effect of KPF_6 addition on ozone generation was investigated, as shown in Fig. 7(a). It is obvious that ozone production increases with KPF_6 addition, as it is 9.6% (with 0.01 M KPF_6 addition) and 16.8% (with 0.05 M KPF_6 addition) higher than that of control (without KPF_6 addition).

It has been reported that the PF_6^- addition can enhance the stability of adsorbed active intermediates (e.g. $^{\bullet}O_{ads}$) on anode surface, such as PbO_2 [12] and Ti/IrO_2-Nb_2O_5 [16] anodes, which contribute to higher ozone production. The $^{\bullet}OH$ adsorbed on anode surface ($^{\bullet}OH_{ads}$) is believed to be an important precursor in the $^{\bullet}O_{ads}$ generation, as listed below [12].

$$H_2O \rightarrow \cdot OH_{ads} + H^+ + e^- \quad (6)$$

$$\cdot OH_{ads} \rightarrow \cdot O_{ads} + H^+ + e^- \quad (7)$$

In the present study, the effect of KPF_6 addition on $^{\bullet}OH$ generation was also investigated (Fig. 7b). It seems that KPF_6 addition has almost no effect on $^{\bullet}OH$ generation on the nanocomposite SnO_2 electrode. Thus, two possible explanations are proposed in the case of KPF_6 addition. One is that the stability of adsorbed active intermediates (e.g. $^{\bullet}O_{ads}$ or $^{\bullet}OH_{ads}$) on the nanocomposite SnO_2 electrode surface is enhanced with KPF_6 addition, which leads to higher ozone production just like PbO_2 [12] and Ti/IrO_2-Nb_2O_5 [16] electrodes. Another explanation is that the trapping reaction of trapping agent with $^{\bullet}OH$ occurs only in bulk solution, and the total $^{\bullet}OH$ (including $^{\bullet}OH$ adsorbed on anode surface and that in bulk solution) with KPF_6 addition might be more than that without KPF_6 addition.

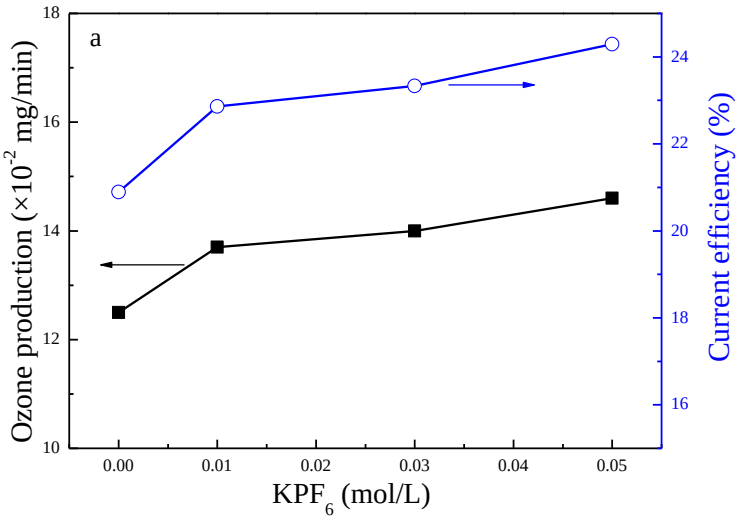

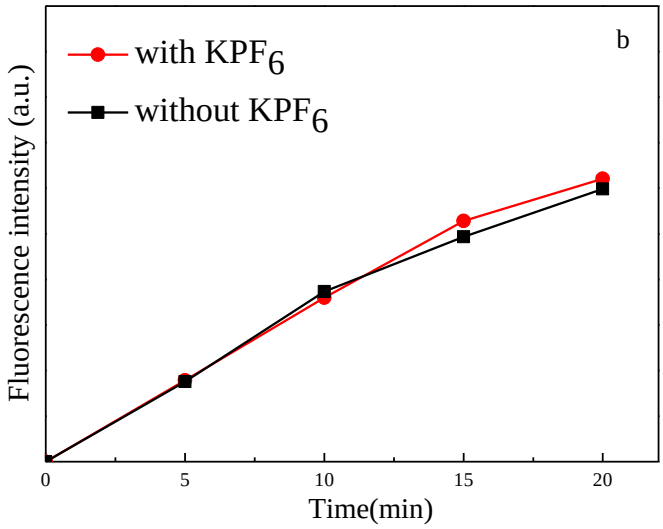

Figure 7. Effect of KPF_6 addition on (a) ozone production and current efficiency. (electrolyte supply = 4.8 mL/s, pH = 2), (b) Effect of KPF_6 addition on hydroxyl radical generation. Na_2SO_4 concentration = 0.25 mol/L, KPF_6 = 0.05 mol/L, current density = 15 mA/cm^2, temperature = 25 ^oC.

3.2 Lifetime and deactivation mechanism of the nanocomposite SnO_2 electrode

To investigate the service life of the prepared nanocomposite SnO_2 electrode, an accelerated life test was conducted and the lifetime of the electrode is estimated as

$$L = \left(\frac{i_t}{i_e}\right)^2 \times t \qquad (3)$$

where L is the lifetime of the electrode (h), i_t is the current density adopted in the accelerated life test (50 mA/cm^2), i_e is the current density adopted in the ozone generation experiment (5 mA/cm^2) and t is the electrolysis time in the accelerated life test (h). In the accelerated life test, the cell voltage increases which implies a deactivation of the working anode. After 63.5 h's electrolysis, the dissolved ozone can hardly be detected, and a 5 V increase of the cell voltage is observed. According to equation (3), the lifetime of the nanocomposite SnO_2 electrode is estimated to be 6350 h. Parsa et al. [38] have reported that a carbon nanotubes (CNT) doped Ti/Sn-Sb-Ni oxide electrode can keep a relatively stable anode potential for at least 17 h in 0.1 M $HClO_4$ at 53.5 mA/cm^2, but they didn't provide its activity variation on ozone generation after the stability test.

The performance of deactivated electrode on $^{\bullet}OH$ generation is compared with that of active electrode, as shown in Fig. 8. It indicates that the $^{\bullet}OH$ production decreases dramatically after the accelerated life test, but a little $^{\bullet}OH$ production still remains on the deactivated nanocomposite SnO_2 electrode, which is not consistent with the ozone production. A reasonable explanation is that the $^{\bullet}OH$ generation from water electrolysis is still ready to occur at high electrode potentials with TiO_2/SnO_2 electrode, as the composition of the deactivated nanocomposite SnO_2 electrode has been investigated (Fig. 10).

The morphology of the nanocomposite SnO_2 electrode before and after accelerated life test was examined by FESEM (Fig. 9). Different from the compact and uniform surface of the freshly prepared electrode (Fig. 9a), the morphology of the electrode after accelerated life test is quite non-uniform like uneven settlement (Fig. 9b). The XRD patterns of the nanocomposite SnO_2 electrode before and after accelerated life test are shown in Fig. 10, and the main diffraction peaks are labelled. A series of diffraction peaks corresponding to rutile type SnO_2 are observed on both of the patterns, and the average crystallite size of SnO_2 is about 10 nm calculated from XRD data using the Scherrer equation. However, compared to the freshly prepared electrode, the intensities of SnO_2 diffraction peaks are significantly weakened on the deactivated electrode after accelerated life test. Besides, there are also diffraction peaks for TiO_2 and Ti in the XRD spectra, while the intensities of both TiO_2 and Ti peaks are found to be much higher on the electrode after accelerated life test than that of the freshly prepared electrode.

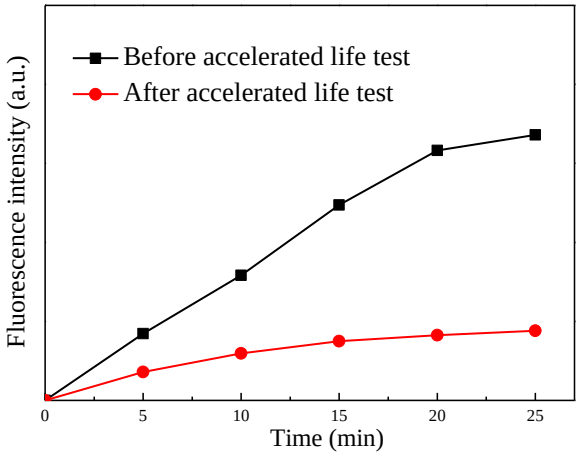

Figure 8. Hydroxyl radical generations on nanocomposite SnO_2 electrode before and after accelerated life test. Na_2SO_4 concentration = 0.25 mol/L, current density = 5 mA/cm^2.

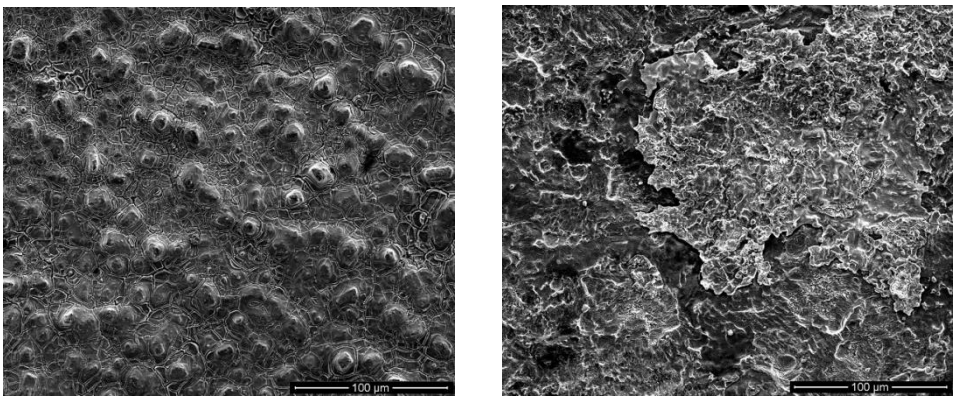

(a) (b)

Figure 9. SEM micrographs of the nanocomposite SnO_2 electrode (a) before and (b) after accelerated life test.

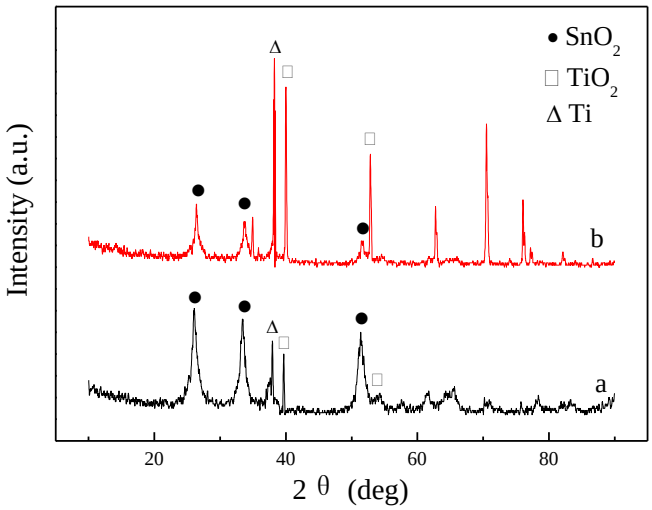

Figure 10. XRD patterns of the nano-composite SnO_2 electrode (a) before and (b) after accelerated life test.

The difference on the XRD spectrum before and after accelerated life test indicates that the SnO_2 coating film on the electrode surface becomes thinner or peels off after long-time electrolysis, while the TiO_2 layer between Ti-base and SnO_2 coating film is growing up in the electrolysis. The destruction of SnO_2 coating film implies a lower loading amount of electrocatalyst, and leads to a loss of electrocatalytic activity of the electrode. The growth of TiO_2 causes the rise of cell voltage since TiO_2 is a poor conductor compared to the doped SnO_2.

4. CONCLUSIONS

Ozone generation on a nanocomposite SnO_2 electrode was investigated. The ozone production and the current efficiency of ozone generation on the nanocomposite SnO_2 electrode are affected by the type of supporting electrolytes and Na_2SO_4 appears to be more suitable for ozone generation than $NaClO_4$, $NaNO_3$ and NaCl. The supporting electrolyte concentration has a complex effect on ozone generation and an optimum concentration of Na_2SO_4 is observed to be 0.25 M. Higher electrolyte supply, lower temperature and lower solution pH favor ozone production and its current efficiency. Higher current density also favors ozone production, while an optimum current density of 5 mA cm^{-2} is obtained for the current efficiency of ozone generation on the nanocomposite SnO_2 electrode. The KPF_6 addition has an obviously positive effect on ozone generation on the nanocomposite SnO_2 electrode as 0.05 M KPF_6 addition can promote 16.8% of ozone production.

The $^{\bullet}OH$ generation in the electrolysis was examined and compared with ozone generation. Higher current density and lower solution pH (in the basic range) is beneficial to $^{\bullet}OH$ production which is in agreement with that of ozone production. Higher temperature also promote $^{\bullet}OH$ production which is inconsistent with that of ozone production. The increased mass transfer process of electrochemical generated $^{\bullet}OH$ from anode surface to bulk solution and the formation of $^{\bullet}OH$ due to the ozone decomposition would contribute to this result. Different from that of ozone production, the

KPF_6 addition has no obvious effect on $^{\bullet}OH$ production in bulk solution, indicating that the addition of KPF_6 only affect adsorbed active species on the nanocomposite SnO_2 electrode.

After accelerated life test, the nanocomposite SnO_2 electrode can hardly produce ozone as well as $^{\bullet}OH$ in the electrolysis. The morphology and XRD analysis on the nanocomposite SnO_2 electrode before and after accelerated life test suggest that the destruction of SnO_2 coating film and the growth of TiO_2 between Ti-base and SnO_2 coating film are responsible for the loss of electrocatalytic activity of this electrode.

ACKNOWLEDGMENTS
This research was supported by the National Nature Science Foundation of China (51008139 and 51378232), the Fundamental Research Funds for the Central Universities (Huazhong University of Science and Technology, 2015QN122) and the Wuhan Youth Chenguang Program of Science and Technology (2014070404010202).

References

1. U. von Gunten, *Water Res.*, 37 (2003) 1443.
2. Z. Q. Liu, J. Ma, Y. H. Cui, L. Zhao and B. P. Zhang, *Appl. Catal. B-Environ.*, 101 (2010) 74.
3. Y. H. Cui, Y. H. Wang, B. Wang, H. H. Zhou, K. Y. Chan and X. Y. Li, *J. Electrochem. Soc.*, 156 (2009) E75.
4. P. A. Christensen, T. Yonar and K. Zakaria, *Ozone-sci. Eng.*, 35 (2013) 149.
5. K. Zakaria and P. A. Christensen, *Electrochim. Acta*, 135 (2014) 11.
6. Y. H. Wang, S. A. Cheng, K. Y. Chan and X. Y. Li, *J. Electrochem. Soc.*, 152 (2005) D197.
7. P. C. Foller and C. W. Tobias, *J. Electrochem. Soc.*, 129 (1982) 506.
8. E. C. G. Rufino, M. H. P. Santana, L. A. De Faria and L. M. Da Silva, *Chem. Pap.*, 64 (2010) 749.
9. M. I. Awad and M. M. Saleh, *J. Solid State Electro.*, 14 (2010) 1877.
10. J. Wang, X. Li, L. Guo and X. Luo, *Appl. Surf. Sci.*, 254 (2008) 6666.
11. A. B. Velichenko, D. V. Girenko, S. V. Kovalyov, A. N. Gnatenko, R. Amadelli and F. I. Danilov, *J. Electroanal. Chem.*, 454 (1998) 203.
12. L. M. Da Silva, L. A. De Faria and J. F. C. Boodts, *Electrochim. Acta*, 48 (2003) 699.
13. R. Amadelli, L. Armelao, A. B. Velichenko, N. V. Nikolenko, D. V. Girenko, S. V. Kovalyov and F. I. Danilov, *Electrochim. Acta*, 45 (1999) 713.
14. T. Ohsaka, M. I. Awad, S. Sata, K. Kaneda, M. Ikematsu, T. Okajima, *Electrochem. Commun.*, 8 (2006) 1263.
15. K. Kitsuka, K. Kaneda, M. Ikematsu, M. Iseki, K. Mushiake and T. Ohsaka, Electrochim. Acta, 55 (2009) 31.
16. M. H. P. Santana, L. A. De Faria and J. F. C. Boodts, *Electrochim. Acta*, 49 (2004) 1925.
17. A. Kraft, M. Tadelmann, M. Wunsche and M. Blaschke, *Electrochem. Commun.*, 8 (2006) 883.
18. K. Arihara, C. Terashima and A. Fujishima, *J. Electrochem. Soc.*, 154 (2007) E71.
19. P. A. Christensen, W. F. Lin, H. Christensen, A. Imkum, J. M. Jin, G. Li and C. M. Dyson, *Ozone-sci. Eng.*, 31 (2009) 287.
20. P. A. Christensen, K. Zakaria, H. Christensen and T. Yonar, *J. Electrochem. Soc.*, 160 (2013) H405.
21. P. A. Christensen, K. Zakaria and T. P. Curtis, *Ozone-sci. Eng.*, 34 (2012) 49.
22. C. Comninellis, *Electrochim. Acta*, 39 (1994) 1857.
23. Y. H. Cui, Y. J. Feng, J. F. Liu and N. Q. Ren, *J. Hazard. Mater.*, 239-240 (2012) 225.
24. Y. H. Cui, Y. J. Feng and Z. Q. Liu, *Electrochim. Acta*, 54 (2009) 4903.

25. G. H. Zhao, Y. G. Zhang, Y. Z. Lei, B. Y. Lv, J. X. Gao, Y. A. Zhang and D. M. Li, *Environ. Sci. Technol.*, 44 (2010) 1754.
26. Y. H. Cui, X. Y. Li and G. H. Chen, *Water Res.*, 43 (2009) 1968.
27. M. Panizza, A. Kapalka and C. Comninellis, *Electrochim. Acta*, 53 (2008) 2289.
28. N. Kishimoto, T. Nakagawa, M. Asano, M. Abe, M. Yamada and Y. Ono, *Water Res.*, 42 (2008) 379.
29. R. Amadelli, L. Samiolo, A. De Battisti and A. B. Velichenko, *J. Electrochem. Soc.*, 158 (2011) P87.
30. Y. H. Cui, Q. Chen, J. Y. Feng and Z. Q. Liu, *RSC Adv.*, 4 (2014) 30471.
31. K. Ishibashi, A. Fujishima, T. Watanabe and K. Hashimoto, *Electrochem. Commun.*, 2 (2000) 207.
32. K. Naya and F. Okada, *Electrochim. Acta*, 78 (2012) 495.
33. A. Kraft, M. Stadelmann, M. Wunsche and M. Blaschke, *Electrochem. Commun.*, 8 (2006) 883.
34. K. Onda, T. Ohba, H. Kusunoki, S. Takezawa, D. Sunakawa and T. Araki, *J. Electrochem. Soc.*, 152 (2005) D177.
35. Y. H. Wang, S. A. Cheng and K. Y. Chan, *Green Chem.*, 8 (2006) 568.
36. P. A. Christensen and A. Imkum, *Ozone-sci. Eng.*, 33 (2011) 389.
37. L. M. Da Silva, L. A. De Faria and J. F. C. Boodts, *Pure Appl. Chem.*, 73 (2001) 1871.
38. J. B. Parsa, M. Abbasi, A. Cornell, *J. Electrochem. Soc.*, 159 (2012) D265.